Macromolecules
ARTICLE

Macromolecules **2009**, *42*, 5179–5188 **5179**
DOI: 10.1021/ma900852r

The Harmony of Helical Macromolecules

Finizia Auriemma* and Claudio De Rosa

Dipartimento di Chimica "Paolo Corradini", Università di Napoli "Federico II", Complesso Monte S.Angelo, Via Cintia, I-80126 Napoli, Italy

Received April 18, 2009; Revised Manuscript Received May 16, 2009

ABSTRACT: The problem of indexing the observed layer lines in fiber diffraction patterns of complex helical structures is illustrated in a comprehensive fashion reviewing the practical aspects of the Cochran, Crick, and Vand theory of helical structures. A practical method that allows indexing the observed layer lines and determining the number of helical residues per turn of the helix is presented. The method is conceptually simple and has the advantage with respect to the literature methods proposed so far (see, for instance, Mitsui in: *Acta Crystallogr.* **1966** *20*, 694 ; *Acta Crystallogr., Sect, A* **1970**, *A26*, 658) of being more suitable for its implementation in a software work-package aimed at solving helical structures. It may be used also by nonspecialists in diffraction analysis of crystalline polymers or even for didactical purposes.

Introduction

Helices are common as preferred conformations in both natural and synthetic macromolecules. Examples of biological molecules with helical structures are polypeptides chains where the α-helix is one of the principal secondary structure in protein,[1] polynucleotides with the double helix of DNA,[2] and polysaccarides.[3] Fibrous proteins often consist of multistrand ropes of α-helices as the double helix of α-keratin[4] and the triple helix of collagen.[5] In addition, in nature, helices are formed at all length scales from the molecular level up to the macroscopic sizes of the plants and animals. Helices are important and ubiquitous in biology because identical objects, regularly assembled, form a helix.[1,6] The phenomenon of coiling, indeed, is observed in various biological and physical systems as it occurs frequently in several supramolecular extended chain aggregates such as actin filaments,[7] myosin filaments,[8] microtubules,[9] amyloid filaments,[10] one-dimensional filaments of bacteria,[11] tobacco mosaic virus,[12] cylindrical stacks of phospholipid membranes interacting with an amphiphilic polymer[13] up to the tendrils of climbing plants.[14]

In the case of synthetic polymers, almost all isotactic and syndiotactic polymers crystallize in helical conformation.[15] Helices are preferred conformations also of polytetrafluoroethylene,[16] polyoxymethylene,[17] and many other important polymers.

Helices consist of periodic one-dimensional objects with periodicity c made up of a structural motif repeating regularly along one axis, trough a translation vector p or "unit height" parallel to the helix axis and a simultaneous rotation t or "unit twist" around the axis. The parameters that characterize the helical repetition of the motif are therefore the helical radius r, and the number of units M and the number of turns N included in the identity period c. The unit height p and the unit twist t are, therefore, defined as the translation along the helix axis per residue and the angle of rotation about the helix axis per residue, respectively. The unit height p and the unit twist t are related to M and N through the relationships:

$$p = \frac{c}{M}; \quad t = \frac{360N}{M}$$

*To whom correspondence should be addressed. Telephone: ++ 39 081 674341. Fax: ++ 39 081 674090. E-mail: finizia.auriemma@unina.it.

Another important parameter used for characterization of helical conformations is the helical pitch P, corresponding to the axial length of the helix in one turn $P = c/N$. Therefore the ratio P/p corresponds to the ratio M/N. If P and p are commensurable, the ratio P/p is rational and may be expressed as the ratio M/N of two integer numbers. As an example, the 3/1 helix of isotactic polypropylene,[15] the 18/5 α-helix of polypeptides,[18] and the 13/6 helix of polytetrafluoroethylene[16] imply repetition of three units in 1 turn, 18 units/5 turns, and 13 units/6 turns, respectively.

The case of helices characterized by a ratio P/p equal to an irrational number implies that it is not possible to find a suitable couple of integer numbers M and N whose ratio is equal to P/p. Complex helices with incommensurable P and p parameters are quite common both in biological macromolecules and synthetic polymers, and arise from small distortions of the P/p ratio from an ideal rational value. In particular, a small twisting of a simple helix characterized by small integer values of M and N parameters may result in a dramatic increase of the chain periodicity c, whereas the P/p value changes only slightly, giving rise to helices with high values of M and N. Noncommensurable helical parameters correspond to helices where each residue advances a distance p parallel to the z (helix) axis and rotates by an angle t around the z axis with p and t remaining finite numbers. Therefore, for helices with noncommensurable P and p parameters the chain repetition period is virtually absent, i.e., $c \rightarrow \infty$, even though the ratio $c/M = p$ is still a finite number.

The conformation of several helical polymers has been determined by considering the effects on the X-ray fiber diffraction patterns caused by helical geometry, exploiting the tendency of polymer substances to form fibers with a high degree of orientation of the helical chains parallel to the fiber axis.[17] The general theory used to perform diffraction analysis of helical structures was first published by Cochran, Crick, and Vand (CCV)[19] for the explicit purpose of explaining the diffraction of X-rays by certain synthetic polypeptides. A version of the formalism was independently developed by Alexander Stokes[20] in the context of the research on the structure of nucleic acids but was published only well after 1951−1953, the crucial years for the discovery of the structure of helical biomolecules.[1,2]

The success of the CCV theory is due to the fact that the theory not only allows for quantitative calculation of the diffraction intensity distribution from helical structures on the different layer

Published on Web 06/05/2009

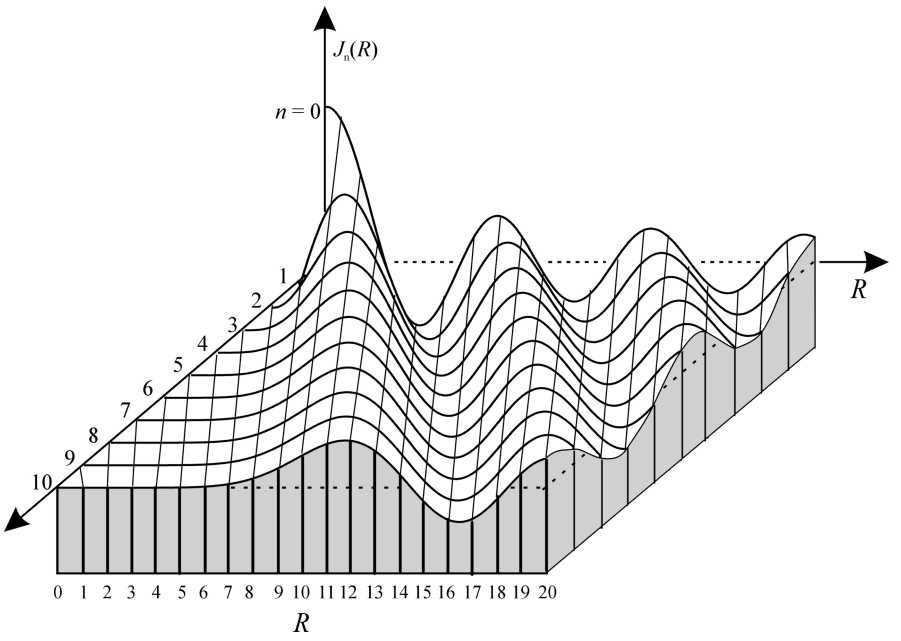

Figure 1. Bessel functions of first kind $J_n(R)$ for n from 0 to 10. We recall that, for negative values of n, the relationship $J_{-n}(R) = (-1)^n J_n(R)$ holds.

lines, but also because it allows for precise determination of helical parameters M and N (or P and p) from analysis of fiber diffraction patterns of well oriented fibrous specimens even in the cases that the exact chemical nature of the diffracting object is unknown.[17]

One of the difficulties encountered in application of CCV theory to extract helical parameters from fiber diffraction patterns consists in the fact that for distorted helices, the interpretation of the fiber diffraction patterns is not straightforward and often may not be performed unambiguously.[21] Since these distortions are quite common both in biological macromolecules and synthetic polymers, different authors have developed their own method to analyze the fiber diffraction patterns from complex helical structure. The most popular and general approach that allows for precise determination of the ratio P/p of a helix is the graphical method proposed by Mitsui.[21a] However, Mitsui's method presents the disadvantage that its application is quite laborious and demanding for its implementation in a software package aimed at solving helical structures.

In this paper, we propose a more direct and simple method for accurate determination of helical parameters, which has the advantage of giving simultaneously all possible trial values of M and N parameters for a correct interpretation of fiber diffraction patterns of complex helices, and allows selecting the most reliable solution. Furthermore the method is more suitable for its implementation in a software work-package aimed at solving helical structures. The method is conceptually simple so that it may be used also by nonspecialists in diffraction analysis of crystalline polymers or simply for didactical purposes.

In the following, after a brief illustration of the CCV theory[19] for the determination of M and N parameters in the case of simple helices, the case of complex helices is presented. Our method is then illustrated and applied to two specific case studies, i.e. poly (γ-methyl-L-glutammate) (PMG)[18] a synthetic polypeptide already studied by Mitsui,[21a] and syndiotactic poly(4-methyl-1-hexene) (sP4MH), a new syndiotactic copolymer produced with a C_s symmetric metallocene catalyst.[22]

Practical Use of the CCV Selection Rule in the Case of Simple Helices

In its essence, the CCV theory establishes that the diffraction intensity on the lth layer line in the X-ray fiber diffraction of a helical structure may be obtained from the square of the structure factor $F(\xi,\psi,l/c)$, which can be calculated from the following equation:

$$F_l\left(\xi, \Psi, \frac{l}{c}\right) = f\left(\xi, \Psi, \frac{l}{c}\right) \sum_n J_n(2\pi\xi r) \exp\left[in\left(\Psi + \frac{\pi}{2}\right)\right] \tag{1}$$

where ξ, ψ and $\zeta = l/c$ are the cylindrical coordinates of a point in reciprocal space, f is the form factor of a helical residue, and J_n is the Bessel function of order n. As shown in the illustration of the Bessel functions of Figure 1, the amplitude of the Bessel function $J_n(X)$ for small values of X decreases rapidly as n increases. The order n of the Bessel functions in the summation is determined according to the selection rule:[19]

$$\zeta = \frac{n}{P} + \frac{m}{p} \tag{2}$$

where m is an integer number. By multiplying both members of eq 2 by c, the selection rule may be also written as:

$$l = mM + nN \tag{2'}$$

The theory demonstrates that the order n of the Bessel functions that contribute to the intensity on each layer line may be found through eq 2 or 2′ by varying m from $-\infty$ to $+\infty$.

As an example, based on eq 2′, the order n of Bessel functions that contribute to the intensity of layer lines l for a 7/2 helix are as follows:

for $l = 0$, $n = \ldots -28, -21, -14, -7, 0, 7, 14, 21, 28, \ldots$
for $l = 1$, $n = \ldots -17, -10, -3, 4, 11, 18, 25, \ldots$
for $l = -1$, $n = \ldots -25, -18, -11, -4, 3, 10, 17, \ldots$
for $l = 2$, $n = \ldots -20, -13, -6, 1, 8, 15, 22, \ldots$
.....
for $l = 7$, $n = \ldots -28, -21, -14, -7, 0, 7, 14, 21, 28, \ldots$
etc.

The difference between successive values of n is always equal to M (i.e., 7 for a 7/2 helix) for each layer line. The high order Bessel functions are small, so only the Bessel functions with $|n| < 7$ make an effective contribution to the diffraction intensity on the

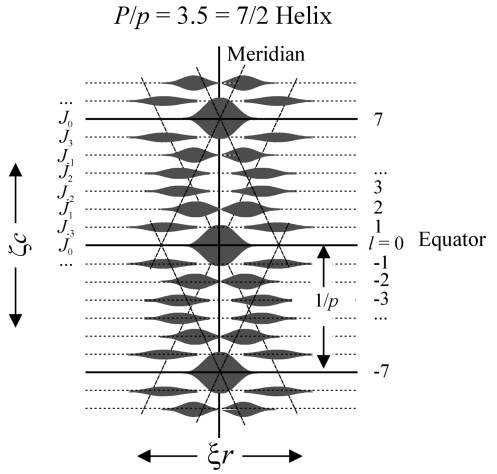

Figure 2. Radial distribution of intensity on the layer lines of a 7/2 helix (of radius r) calculated taking into account only the first maximum of the lowest order Bessel function. The Bessel functions J_n of lowest order that contribute to the intensity on the different layer lines are indicated. The intensity is a continuous function along the radial cylindrical coordinate ξ and is nonzero only at heights ζ of reciprocal space equal to l/c with l an integer number corresponding to the index of the layer lines.

layer lines at radial distance from the meridian of practical interest for polymers.

Furthermore, one should consider that only the zero-order Bessel function shows a maximum at the origin (Figure 1), whereas for the Bessel functions with $n > 0$ the height of the first principal maximum gradually decreases with increasing n, and its location becomes displaced from the origin by an amount that increases with n (Figure 1).

The distribution of the intensity due exclusively to the main peak of the lowest order Bessel function that contributes to the structure factor on the various layer lines for a 7/2 helix is shown in Figure 2.

It is apparent that aside the equator, a meridional maximum is present on layer lines with l equal to a multiple of 7, where the zero order Bessel function contributes. It is also apparent that the strongest intensity layer lines aside those with a meridional maximum are those with $l = \pm 2, \pm 5, \pm 9, \pm 12, ...$, i.e. with $l = (\pm m7 \pm 2)$, where the first order Bessel function contributes. Moreover, the higher the lowest order of the Bessel function contributing to the scattered intensity on a given layer, the more displaced from the meridian axis is the position of the main maximum. Simulated fiber diffraction patterns of helices of the kind shown in Figure 2 may be obtained using the program HELIX by Knupp and Squire[23] whose version running under Microsoft Windows, is freely available at the CCP13 Web site (http://www.ccp13.ac.uk).

More generally, for a M/N helix, based on the selection rule 2 and/or 2′, strong meridional reflections are generally expected on layer lines with $l = \pm mc/p = \pm mM$, where the zero-order Bessel function contributes. Furthermore the diffraction intensity in zones of reciprocal space close to the meridian (at low ξ value) is higher the lower the order of Bessel functions contributing to the structure factor.

These general "rules" have been exploited in the common practice in many cases to analyze the fiber diffraction patterns of helical structures, with the aim of finding confident values of the helical parameters M and N (or P and p), to be used in the successive steps of structural analysis, that is, for building molecular models of the conformation and packing of the chains and then for performing structure factors calculations to be compared with the experimental diffraction intensities. In other terms, although for structures containing more than one atom per residue and/or more than one helix per unit cell the distribution of diffraction intensity on the layer lines depends also on the relative phases of all atoms (for quantitative calculation of the radial distribution of intensity of helical structures see for instance refs 17 and 19), it is possible to find confident values of the helical parameters M and N (or P and p) only taking into account for each layer line the experimental values of ζ_{obs} and the average diffraction intensity estimated on a qualitative or semiquantitative basis in regions close to the meridian from the fiber diffraction patterns of well-oriented fiber specimens of a polymer sample.

Table 1. Average Values of the Diffraction Intensity (I_{obs}) on the Various Layer Lines l Having Experimental Cylindrical Coordinates ζ_{obs} Observed in the X-ray Fiber Diffraction Pattern of Form I of Isotactic Poly(4-methyl-1-pentene)[24] and Absolute Values of the Lowest Order of the Bessel Functions n That Contribute to the Diffraction Intensity on the Layer Lines for Hypothetical 7/N Helices with N = 1 (or 6), 2 (or 5), and 3 (or 4)

experimental			lowest order $\|n\|$ of Bessel functions for M/N helices[a]		
ζ_{obs} (Å^{-1})	l	I_{obs}	7/1, 7/6	7/2, 7/5	7/3, 7/4
0	0	strong	0	0	0
0.072	1	weak	1	3	2
0.145	2	strong	2	1	3
0.217	3	medium	3	2	1
0.290	4	medium	3	2	1
0.362	5	strong	2	1	3
0.435	6	weak	1	3	2
0.507	7	strong[b]	0	0	0

[a] For each pair of enantiomorphic helices, that is 7/1 and 7/6, 7/2 and 7/5, and 7/3 and 7/4 the value $|n|$ of the lowest order Bessel function contributing the intensity on the layer line is given in absolute value. [b] Meridional reflection.

As an example of application of the Cochran, Crick and Vand selection rule, the case of form I of isotactic poly(4-methyl-1-pentene) (iP4MP) is illustrated.[24] The experimental values of the height ζ_{obs} of the layer lines observed in the X-ray fiber diffraction pattern of iP4MP along with a qualitative estimation of the observed intensity on the first seven layer lines beside the equator are listed in Table 1.[24] As reported in ref 24, the heights ζ_{obs} of the layer lines can be interpreted in terms of a chain periodicity c of 13.80 Å. The isotactic configuration of the chain (see ref 15) suggests that the chain conformation is helical. The presence of a meridional reflection on the 7-th layer line indicates that the crystal structure of iP4MP may be described in terms of chains in helical conformation characterized by $M = 7$ residues included in the identity period. The comparison between the intensity of reflections observed on the various layer lines and the lowest order of the Bessel functions that contribute to the theoretical diffraction intensity on the various layer lines of the possible 7/N helices, according to the CCV theory and the selection rules 2, 2′, is reported in Table 1, for N = 1, 2, and 3, corresponding to the helices 7/1, 7/2, and 7/3, and $N = 6$, 5, and 4 for the corresponding $M/(M-N)$ enantiomorphic helices 7/6, 7/5, and 7/4, respectively. The data of Table 1 clearly indicate that the 7/2 helix, or/and 7/5 helix, gives a distribution of lowest order of the Bessel functions on the layer lines in best agreement with the experimental intensities.

This practice has been used in a large number of cases independent of the number of atoms in a helical residue, and the number of helices per unit cell. The so inferred 7/2 helix of form I of iP4MP has been effectively confirmed in the successive steps of diffraction analysis even though the unit cell includes more than one helix.[24]

Complex Helices

As discussed in the Introduction for the case where the ratio P/p is an irrational number, the chain periodicity is virtually absent, that is $c \rightarrow \infty$, so that the layer lines become infinitely close each other. Therefore, for a helix with incommensurable parameters, planes at height $\zeta = n/P + m/p$ fill the whole reciprocal space, and the layer spacing $c^* = 1/c$ becomes small as c increases and in the limit of $c \rightarrow \infty$, $c^* \rightarrow 0$. In practice, as demonstrated in the original paper by CCV[19] it is possible to approximate the true values of P/p by some rational fraction $P'/p' = M/N$, which accounts for all the features of the diffraction pattern. This practice may be justified by the following argument. Let us write in explicit the selection rule for a true helix (helical parameters P and p) and an approximate helix (helical parameters P' and p'):

$$\zeta = \frac{n}{P} + \frac{m}{p} \tag{3}$$

and

$$\zeta' = \frac{n}{P'} + \frac{m}{p'} \tag{4}$$

Using the approximate values P' and p', a given Bessel function, whose position along ζ is defined by m and n, moves in the reciprocal space by a quantity $\Delta\zeta = \zeta - \zeta'$:

$$\zeta - \zeta' = \Delta\zeta = n\left(\frac{1}{P} - \frac{1}{P'}\right) + m\left(\frac{1}{p} - \frac{1}{p'}\right) = n\frac{\Delta P}{PP'} + m\frac{\Delta p}{pp'} \tag{5}$$

According to eq 5, if the deviations ΔP and Δp are small, the Bessel function in question will move only a small distance in the reciprocal space $\Delta\zeta$, especially if n and m are also small. With increasing the identity period c, the number of structural units included in the identity period M also increases and the Bessel functions that for a simpler helix contribute to the diffraction intensity on the same layer line ζ, are split on different layer lines and the closely spaced layer lines become mostly filled by Bessel functions of high order. Therefore, for the majority of the layer lines, the intensity is quite small, and the lowest order Bessel functions remain confined in layer lines close to positions given by the simple helix corresponding to the commensurable approximation of P and p.

These concepts are illustrated in Figure 3, as an example. Let us suppose that a 5/2 helix is slightly distorted so that, it is characterized by ≈2.47 residues per turn, instead of 2.5. This distortion corresponds to a helix including 5 residues in ≈ 5/2.47 ≈ 2.02 turns instead of 2 turns. The most trivial solution of integer values of M and N is of course a 247/100 helix. The heights ζ of layer lines where the Bessel functions of order less than 5 contribute to the diffraction intensity for a 247/100 helix are shown in Figure 3D. It is apparent that the Bessel functions that for the 5/2 helix contribute to the diffraction intensity on the same layer line, e.g. J_{-2} and J_3 for $l = 1$, J_1 and J_{-4} for $l = 2$, J_{-1} and J_4 for $l = 3$, etc. (Figure 3A), are split on different layer lines in the case of the 247/100 helix, e.g. J_{-2} for $l = 47$ and J_3 for $l = 53$, J_1 for $l = 100$ and J_{-4} for $l = 94$, etc. (Figure 3D). Therefore, the first layer line for the simple 5/2 helix at $\zeta = 1/c$ becomes the 47th and 53th layer lines at $\zeta = 47/c'$ and $53/c'$, respectively, and the reciprocal space between the equator $l = 0$ ($\zeta = 0$) and the first layer line of the 5/2 helix ($\zeta = 1/c$), where non-negligible diffraction intensity is concentrated, becomes filled by 46 closely spaced layer lines where a low diffraction intensity is concentrated, due to the contribution of Bessel functions of high order (Figure 3D). Therefore, for the 247/100 helix the intensity remains namely concentrated at ζ values ($\zeta = 47/c'$, $53/c'$, $94/c'$, $100/c'$ ... and $247/c'$) close to the heights ζ of the parent (undistorted) 5/2 helix ($\zeta = 1/c$, $2/c$, $3/c$, $4/c$, and $5/c$).

Figure 3 also shows the concept that the main features of the diffraction pattern of a complex helix are already contained in a less complex approximation, namely the 42/17 helix (Figure 3C) or the 37/15 helix (Figure 3B), since they correspond to the same distribution of the lowest order Bessel function on the layer lines as the 247/100 helix. For instance, for the 37/15 helix the Bessel functions of low order J_{-2} and J_3 define the diffraction intensity on the 7th and 8th layer lines, respectively, close to the 47th and

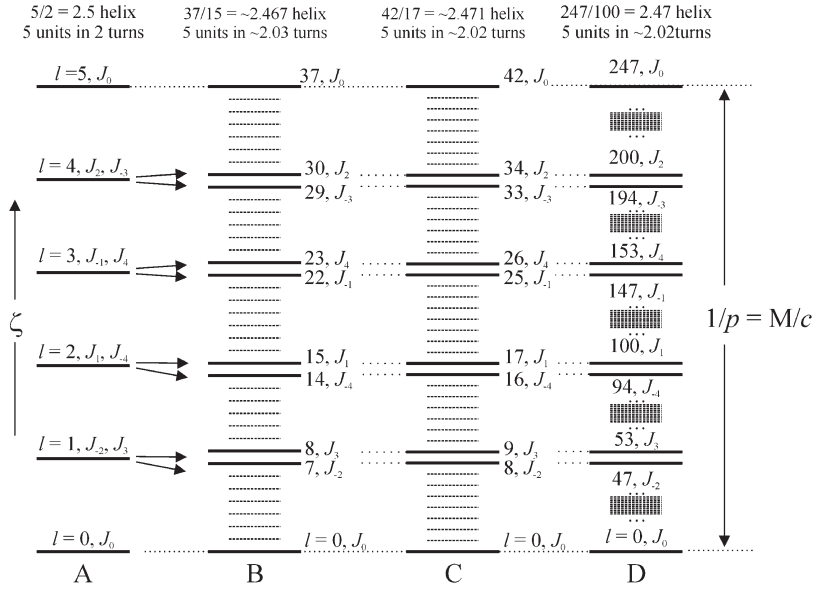

Figure 3. Distribution along the ζ axis of the lowest order Bessel functions that contribute to the diffraction intensity on the indicated layer lines l for 5/2 (A), 37/15 (B), 42/17 (C), and 247/100 (D) helices, corresponding to the same value of unit height $p = c/M$. Only the Bessel functions with $|n| < 5$ are considered. The complex helices B−D may be considered as resulting from small distortions (twisting) of the 5/2 helix, and correspond to helices characterized by 5 residues in ≈2.02−2.03 turns, instead than in 2 turns. Since strong meridional reflections are generally expected on layer lines with $l = M$, where the zero-order Bessel function contributes, $\zeta_{\text{meridional}} = M/c = 1/p$.

53th layer lines of the more complex 247/100 helix, the Bessel functions J_1 and J_{-4} define the intensity on the 14th and 15th layer lines, close to the 94th and 100th layer lines of the 247/100 helix, etc. (Figure 3B). In other terms the important Bessel functions of low order of a incommensurate helix are confined in layer lines close to positions given by simpler helices corresponding to commensurable approximations of P and p, the precision in the determination of P and p being limited by the experimental error.

In general, from the experimental ratio P/p of a given helix the first nontrivial commensurable helical approximation (with the lowest M and N integer number) may be found with M the smallest possible integer number multiple of P/p whereas the values of N is calculated from $N = M/(P/p)$.

Therefore, in diffraction analysis of complex helical structures, a practical difficulty in precise determination of helical parameters arises because a small twisting of the helix may result in a dramatic change of the chain periodicity c, whereas the P/p value changes only slightly. In fact, large values of c while p remains close to the corresponding value of undistorted helix ($p \ll c$), correspond to large values of $M = c/p$, so that it is not easy to index the layer lines without ambiguity because low order Bessel functions contribute to the diffraction intensity of only a small number of layer lines, whose l indices do not vary with continuity. A further complication arises from the broadness of layer lines along ζ, because twisting of a simple helix is often associated with conformational disorder due to local variations of P and p. Also in this case the diffuse scattering is concentrated close to the layer lines where the lowest Bessel functions contribute, and this occurs in regions of reciprocal space corresponding to the average values of P and p.

A precise determination of the ratio P/p may be obtained resorting to the graphical method proposed by Mitsui.[21] To this aim, selection rule 2 is rewritten, multiplying both sides by P or p to obtain the following equations:

$$\zeta_{rel} = \zeta P = n + m\frac{P}{p} \tag{6}$$

or

$$\zeta'_{rel} = \zeta p = n\frac{p}{P} + m \tag{7}$$

Equations 6 and 7, define two reduced variables ζ_{rel} and ζ'_{rel} and allow building the diagrams of the kind shown in Figure 4, in the case of eq 7. Close to each straight line the order n of the Bessel function is indicated, whereas the exact value of m is not indicated because it does not affect the diffraction intensity distribution directly. From this kind of diagrams it is possible to visualize the change of the distribution of the diffraction intensity as a function of the ratio p/P (Figure 4), or P/p if eq 6 is used.

Since the relative positions of the layer lines corresponding to higher order Bessel functions are more sensitive to the changes of P/p and p/P, the plots of Figure 4 can be utilized for an accurate determination of helical parameters. The application of this method is exemplified in the case of some synthetic α-polypetides in the plot of Figure 4, which is redrawn from Figure 3 of the original paper of Mitsui.[21] A possible procedure for the use of the diagram ζ'_{rel} vs. p/P (Figure 4) is as follows:

(a) Plot the observed values of ζ, determined from the X-ray fiber diffraction pattern, on a transparent paper after scaling by multiplication for the experimental value of the unit height p. Mark the relative intensities of the layer lines.

(b) Set the transparent paper parallel to the ordinate of the plot of Figure 4, and try to find the best fit by sliding the paper along the p/P-axis, until a satisfactory agreement between the observed spacing of the layer lines along ζ'_{rel} and a reasonable correspondence of the order n of the Bessel function to the relative intensities are obtained.

(c) The so obtained value of the p/P ratio is used to find a suitable commensurable nontrivial approximation of the M and N parameters. Once the (m, n) values have been assigned to each layer, the index l of the layer line can be calculated using the selection rule 2. The identity period c may be then calculated as the weighted average of l/ζ_{obs}.

The application of the Mitsui method[21] is here illustrated in some detail in the case of poly(γ-methyl-L-glutammate) (PMG). For the chains of PMG various helical conformations having $P/p \approx 3.63$ have been proposed, i.e. the 29/8 (=3.625), 98/27 (=3.630), 69/19 (=3.631), and 91/25 (=3.640) helices.[18] The plot of Figure 4 readily shows that the experimental distribution of intensity on the layer lines is in a better agreement with the distribution of Bessel functions for helices with $P/p = 3.61$. From this value the chain periodicity $c = 97.26$ Å was proposed by Mitsui,[21a] by assuming a 65/18 (=3.611) helix. The observed values of the height ζ_{obs} of the layer lines of PMG are compared in Table 2 with those calculated (ζ_{calc}) in the case of 18/5, 29/8, 47/13 and 65/18 helices. It is apparent the better agreement between ζ_{obs} and ζ_{calc} achieved for 65/18 helix proposed by Mitsui.[21a]

The New Method

We propose a more direct and simple method for accurate determination of helical parameters, which has the advantage of giving simultaneously all possible solutions and it is more suitable for the implementation in a software work-package for solving helical structures. The method consists in performing an indexing of the observed layer lines by evaluating for each observed value of ζ_{obs} trial values of the identity period c, as $c = l/\zeta_{obs}$ with l an integer number corresponding to the trial value of the index l of the layer line. Solutions are selected among those that allow indexing all observed layer lines for identical values of c within the experimental error.

The problem may be formally stated by solving the following system of discrete equations, using the identity period c as a parameter.

$$\begin{cases} \zeta_1^{-1} l_1 = c \\ \zeta_2^{-1} l_2 = c \\ \cdots\cdots\cdots\cdots \\ \zeta_n^{-1} l_n = c \end{cases} \tag{8}$$

The system shown in eq 8 may be reformatted to a matrix formula that is suitable for electronic computing:

$$(\mathbf{ZE})^{-1}\mathbf{L} = c\mathbf{J} \tag{9}$$

where $\mathbf{Z}$ is the row vector of order $1 \times k$ whose elements are the observed values of ζ (the ζ_{obs} values), $\mathbf{E}$ is the unit matrix of order $k \times k$, $\mathbf{L}$ is the column vector of order k whose elements are the values of l that allow for indexing the observed layer lines, c is the parametric variable corresponding to the identity period of the chain and $\mathbf{J}$ is the column vector of order k whose elements are equal to 1. Equation 9 is numerically solved admitting as solutions only the values of c for which the elements of the column vector $\mathbf{L}$ are integer numbers.

The method is graphically illustrated in the case of PMG in Figure 5. Taking in consideration only the indexing schemes for which the weighted average value of the chain periodicity c is less than 100 Å, and the standard deviation from this average is below a threshold, the most likely solutions are delineated by the dotted horizontal lines in Figure 5A. For instance, the trial values of $l =$ 2, 3, 5, 8, and 18, corresponding to the observed values of ζ of Table 2 allow indexing the observed layer lines for an identical value of $c = 26.9$ Å. The other three solutions corresponding to the horizontal lines in Figure 5A are those already reported

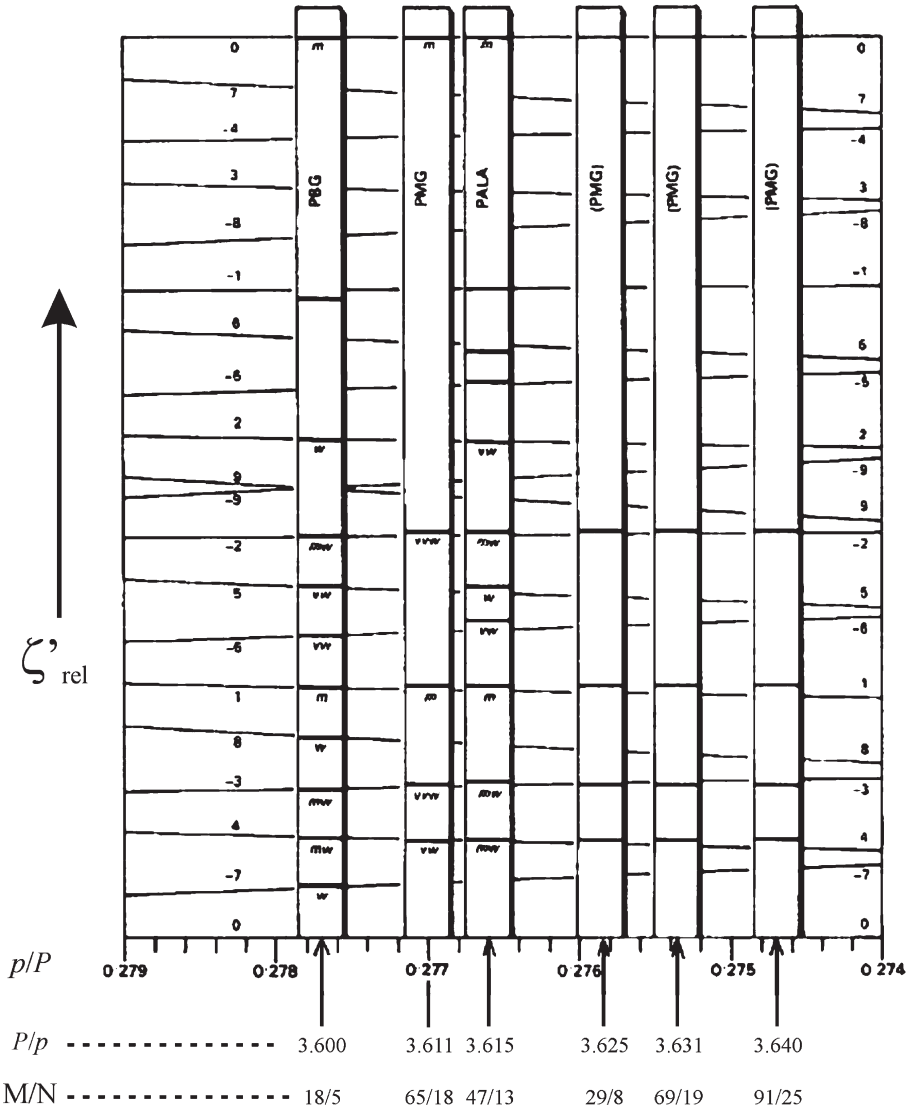

Figure 4. $\zeta'_{rel}-p/P$ diagram applied to the α-helices of some synthetic polypeptides (redrawn from ref 21a). The number on the straight lines indicates the order of the Bessel functions that contribute to the diffraction intensity on the layer lines corresponding to the values of $\zeta'_{rel} = \zeta\, p$. The relative experimental intensities (very weak (vw), weak (w), medium (m), medium weak (mw)) observed on the layer line ζ for poly(γ-butyl-L-glutammate) (PBG), poly(γ-methyl-L-glutammate) (PMG), and poly(L-alanine) PALA are marked on the strips.

Table 2. Comparison of Possible Indexing Schemes of Layer Lines *l* for Poly(γ-methyl-L-glutamate)[21a]

experimental data		18/5 helix, c = 26.9 Å, P/p = 3.6		29/8 helix, c = 43.2 Å, P/p = 3.625		47/13 helix, c = 70.0 Å, P/p = 3.615		65/18 helix, c = 97.2 Å, P/p = 3.611		
ζ_{obs}(Å^{-1})[a]	intensity[b]	l	ζ_{calc} (Å^{-1})[a]	l	ζ_{calc}(Å^{-1})[a]	l	ζ_{calc}(Å^{-1})[a]	l	ζ_{calc}(Å^{-1})[a]	n[c]
0	m	0	0	0	0	0	0	0	0	0
0.070_7	vw	2	0.074_3	3	0.069_4	5	0.071_4	7	0.072_0	+4
0.112_2	vvw	3	0.111_5	5	0.115_7	8	0.114_2	11	0.113_1	−3
0.185_8	m	5	0.185_9	8	0.185_1	13	0.185_7	18	0.185_1	+1
0.299_0	vvw	8	0.297_4	13	0.300_8	21	0.300_1	29	0.298_1	−2
0.668_9	m	18	0.669_1	29	0.671_1	47	0.671_4	65	0.668_3	0

[a] Observed values of the cylindrical coordinate ζ (ζ_{obs}) of the different layer lines in the X-ray fiber diffraction pattern of PMG and values calculated (ζ_{calc}) for helices 18/5, 29/8, 47/13, and 65/18. [b] Average value of the experimental diffraction intensity observed on the various layer lines l of the X-ray fiber diffraction pattern of PMG. Key: m = medium, vw = very weak, and vvw = very very weak. [c] Value of the lowest order n of the Bessel functions that contribute to the diffraction intensity on the corresponding layer line at the value of ζ_{calc}.

in Table 2; the fourth one is the conformation proposed by Mitsui,[21a] where the trial values of l = 7, 11, 18, 29, and 65 allow indexing the observed layer lines for an identical value of c = 97.2 Å (Figure 5A). Therefore, this method allows indexing all the layer lines with integer numbers in a satisfactory way, according to several possible solutions.

Extension of the diagram of Figure 5A to solutions leading to values of chain periodicity c higher than 100 Å is straightforward. Therefore, the possible indexing schemes of the observed layer lines found in any chosen interval of values of c, identify a set of possible solutions to the problem of indexing the diffraction pattern of a helical structure. These solutions are consequently

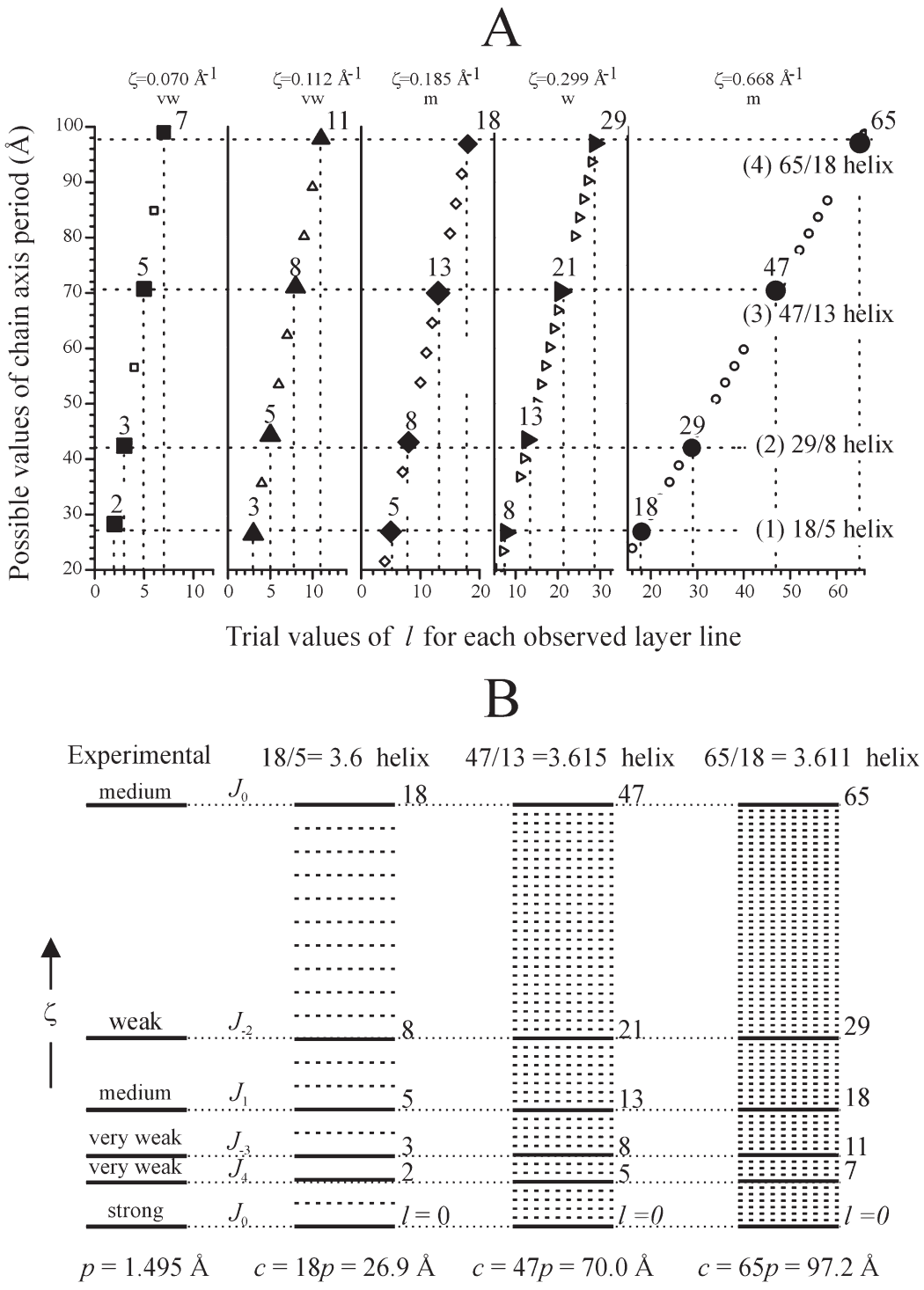

Figure 5. (A) Graphical solution of parametric discrete system of eqs 8 and 9, for indexing the observed layer lines of a fiber diffraction pattern of a helical structure in the case of PMG. For each observed layer line, corresponding to the experimental values of ζ, the possible values of the identity period c are plotted as a function of the trial values of the index l. The solutions (1−4) are delineated by the dotted horizontal lines that correspond to a possible indexing of the observed layer lines for an identical value of c. (B) Experimental diffraction intensity on the observed layer line in the X-ray fiber diffraction pattern of PMG and comparison with the lowest order Bessel functions that contribute to the calculated diffraction intensity on the layer lines for the 18/5, 47/13, and 65/18 helices. For these helices the distribution of the lowest order Bessel functions is in qualitative agreement with the experimental distribution of intensity on the layer lines. For helices with incommensurable P and p parameters, the observed layer lines may be indexed according to an infinite number of schemes, and solutions 2−4 (29/8, 47/13, and 65/18 helices, respectively) correspond to distorted 18/5 (= 3.6) α-helices typical of polypeptides.[1,18].

labeled according to the increasing value of c or some other criterion, for instance using the standard deviation (σ) of the observed layer line spacings from calculated value as a merit figure.

In the successive step, for any given solution labeled i, characterized by a value of the chain periodicity c_i, the corresponding values of helical parameters M_i and N_i are found, exploiting all additional available structural information. In particular knowing the value of unit height p, the value of M_i is calculated as the nearest integer number (n_{int}) close to the ratio $M_i = n_{int}(c_i/p)$. The value of N_i is then established by trial and error, applying the selection rule 2′ to find for all possible values

Table 3. Average Values of the Diffraction Intensity (I_{obs}) on the Various Layer Lines *l* Having Experimental Cylindrical Coordinates ζ_{obs} Observed in the X-ray Fiber Diffraction Pattern of Syndiotactic Poly(4-methyl-1-hexene), and Lowest Order of the Bessel Functions *n* That Contribute to the Diffraction Intensity on the Layer Lines for Hypothetical Helices 17/*N* and 22/*N*[a] for Different Values of *n*

experimental		lowest order |*n*| of Bessel functions for *M*/*N* helices							
ζ_{obs} (Å^{-1})	I_{obs}[b]	*l*	17/3 17/14	17/4 17/13	17/6 17/11	17/7 17/10	*l*	22/5 22/17	22/9 22/11
0	s	0	0	0	0	0	0	0	0
0.045	w	3	1	5	8	2	4	8	2
0.056	m	4	7	1	5	3	5	1	3
0.091	w	6	2	7	1	4	8	6	4
0.101	s	7	8	6	4	1	9	7	1
0.147	vs	10	8	6	4	1	13	7	1
0.159	w	11	2	7	1	4	14	6	4
0.202	s	14	1	5	8	2	18	8	2
0.248	ms	17	0	0	0	0	22	0	0

[a] The couples of enantiomorphic helices 22/4 = 11/2 and 22/18 = 11/9, 22/8 = 11/4, and 22/14 = 11/7 are not considered because they correspond to helices whose periodicity $c = 11\,p = 44.0_3$ is not a solution of the discrete system of eqs 8 and 9. [b] Key: vs = very strong, s = strong, ms = medium strong, m = medium, and w = weak.

of N_i the lowest order Bessel function that contributes to the diffraction intensity on each layer line. In this procedure the possible values for N_i are chosen numerically coincident with the values of *l* that index the observed layer lines for the *i*-th solution. At this stage of analysis M_i/N_i helices with M_i and N_i values having a common factor should be discarded, because they identify solutions for which the chain periodicity *c* corresponds to $c = c_i/K$ with *K* the greatest common factor between M_i and N_i. The most reliable M_i/N_i helix is then identified as the helix that gives a distribution of the lowest order Bessel function on the various layer lines in the best qualitative agreement with the experimental intensity distribution, and that gives the best agreement between the observed (ζ_{obs}) and calculated (ζ_{calc}) values of the height of the various layer lines ζ. Following this procedure, solution 4 in Figure 5A corresponds to the 65/18 helix proposed by Mitsui,[21a] and gives the best agreement. However, application of this method confirms that the other solutions are good approximations for the conformation of the chain of PMG. It is apparent, indeed, from Figure 5 that an additional good approximate solution of the incommensurable helical conformation of PMG may be envisaged in the 47/13 (=3.615) helix and that all possible solutions envisaged in Figure 5 and in Table 2 correspond to a distorted 18/5 α-helix, typical of polypeptides.[1,18]

As an example of application of the proposed method to a crystalline polymer whose conformation of the chain and the crystal structure are still unknown, the case of syndiotactic poly (4-methyl-1-hexene) (sP4MH) is explicitly illustrated. sP4MH has been prepared with a syndiospecific C_s-symmetric metallocene catalyst[22] and shows a melting temperature of 166 °C. The diffraction intensity of fiber specimens of sP4MH is distributed over 8 off-equatorial layer lines whose heights ζ_{obs} are reported in Table 3. The presence of a meridional reflection on the 8-th observed layer line at $\zeta_{obs} = 0.248_0$ Å^{-1} gives a value of the unit height $p = 4.03_3$ Å (since strong meridional reflections are generally expected on layer lines with $l = M$, where the zero-order Bessel function contributes, $\zeta_{meridional} = M/c = 1/p$ and $p = 1/\zeta_{meridional} = 1/0.248_3$). The indexing of the observed layer lines is nontrivial, indicating that the conformation corresponds to a complex helix.

The application of our method to the diffraction data of sP4MH of Table 3 is shown in Figure 6. Also in this case, taking in consideration only the indexing schemes for which the weighted average value of the chain periodicity *c* is less than 100 Å, the most likely solutions of the eqs 8 and 9 are delineated by the dotted horizontal lines in Figure 6A (solutions 1−3). According to the solution n.1 the possible values of *l* indices for the observed nonequatorial layer lines are *l* = 2, 3, 4, 5, 7, 8, 10, and 12, for an identical value of the chain periodicity $c \approx 48 \pm 3$ Å, corresponding to helices including $M = c/p \approx 48/4.03 \approx 12$ residues per period. Similarly, the solution *n*.2 corresponds to an indexing of the off-equatorial layer lines with *l* = 3, 4, 6, 7, 10, 11, 14, 17 for a chain periodicity $c \approx 69 \pm 2$ Å, corresponding to helices including $M = c/p \approx 69/4.03 \approx 17$ residues per period. Finally, for the solution n.3 the *l* indices of the observed layer lines are *l* = 4, 5, 8, 9, 13, 14, 18, 22, the chain periodicity *c* corresponds to $c = \approx 88.7 \pm 0.5$ Å and the crystal structure would be described by helices with $M = c/p \approx 89/4.03 \approx 22$ residues per period.

According to the described procedure, the values of *N* for each solution are established by trial and error, applying selection rule 2′ to find for all possible values of *N* the lowest order Bessel function that contributes to the diffraction intensity on each layer line. The most reliable *M*/*N* helix is then identified as the helix that gives a distribution of the lowest order Bessel function on the various layer lines in the best qualitative agreement with the experimental intensity distribution, with *M* and *N* relatively prime numbers. Let us consider the second indexing scheme of the observed layer line for which *M* = 17. Possible helices with *M* = 17 that lead to a nonnegligible diffraction intensity on the observed layer line of sP4MH are the enantiomorphic couples 17/3 and 17/14, 17/4 and 17/13, 17/6 and 17/11, and 17/7 and 17/10 (Table 3). Application of the selection rule 2′ indicates that the distribution of the lowest order Bessel functions on the observed layer lines in the best qualitative agreement with the experimental intensity distribution is obtained for the couple of enantiomorphic helices 17/7 ≈ 2.43 and 17/10 (Table 3). Similar analysis is reported in Table 3 for the third indexing scheme of Figure 6A for which *M* = 22. In this case the couples of enantiomorphic helices 22/4 and 22/18, 22/8 and 22/14 are discarded since they correspond to 11/2 and 11/9, 11/4 and 11/7 helices, respectively, whose periodicity $c = 11\,p = 44.0_3$ is not a solution of the system of eqs 8 and 9. Nonnegligible intensities on the layer lines are obtained for the couple of enantiomorphic helices 22/5 and 22/17, 22/9 and 22/13. It is apparent that a distribution of the lowest order Bessel functions on the observed layer lines in good qualitative agreement with the experimental distribution of intensity is obtained for the 22/9 ≈ 2.44 helix (or the enantiomorphous 22/13 helix) (Table 3).

Similar considerations lead to identify the helix with *M*/*N* = 12/5 (= 2.4) for the indexing scheme corresponding to the solution n.1 (Figure 6A). Therefore, a suitable description for the helical conformation of sP4MH in the crystals corresponds to *M*/*N* ratio ≈ 2.4, that is to a 12/5 (=2.4) helix for the solution n.1 with $c = 12p = 48.3$ Å, a 17/7 (≈ 2.43) helix for the solution *n*.2 with $c = 17p = 66.6$ Å, and a 22/9 (≈ 2.44) helix for the solution *n*.3 with $c = 22p = 88.7$ Å (Figure 6B). The 17/7 and 22/9 helices, indeed, correspond to a slight distortion of the 12/5 (= 2.4) helix with $c = 12p = 48.3$ Å (the solution numbered

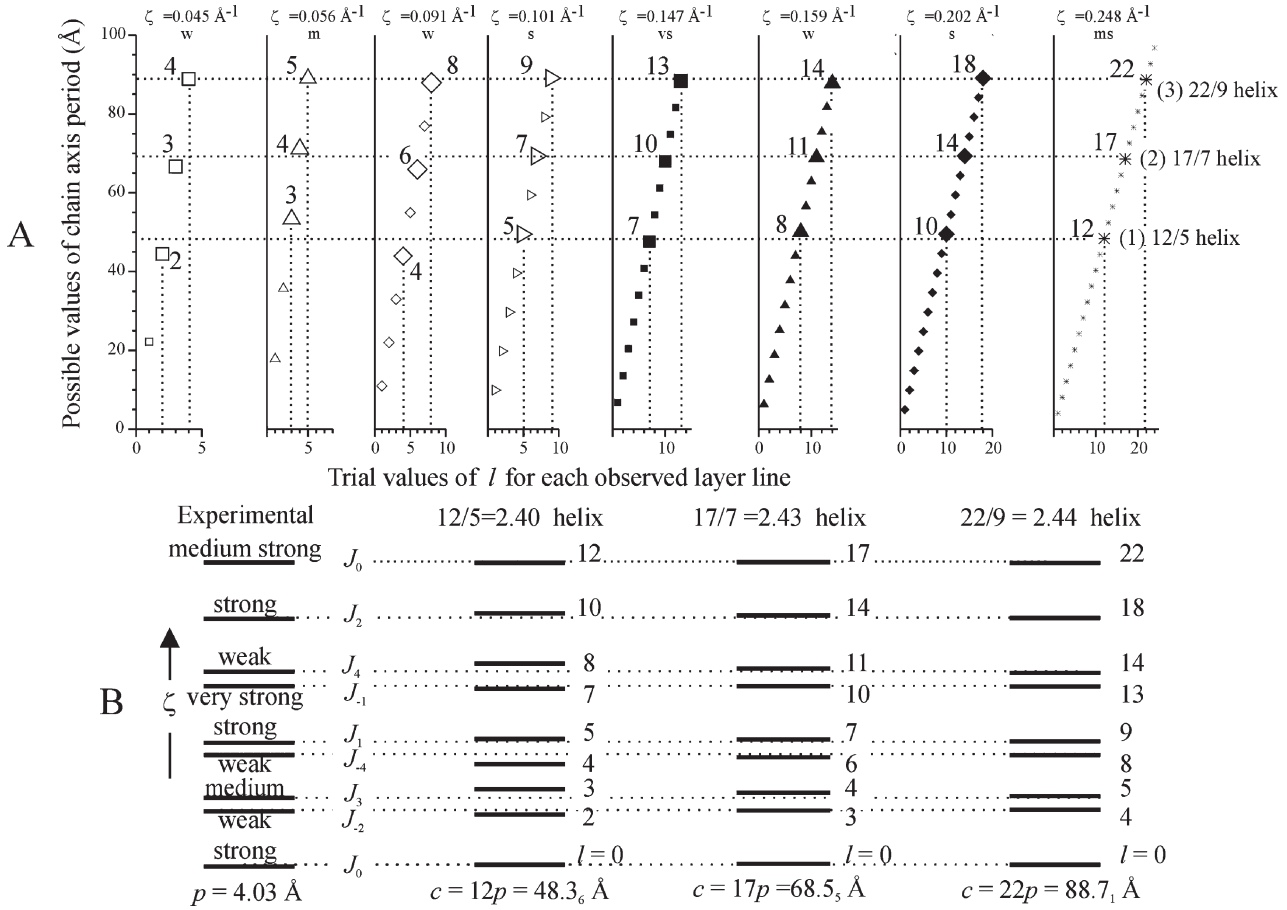

Figure 6. (A) Graphical solution of parametric discrete system of eqs 8 and 9, for indexing the observed layer lines in the fiber diffraction pattern of syndiotactic poly(4-methyl-1-hexene). For each observed layer line, corresponding to the experimental values of ζ, the possible values of the identity period *c* are plotted as a function of the trial values of the index *l*. The solutions (1−3) are delineated by the dotted horizontal lines that correspond to a possible indexing of the observed layer lines for an identical value of *c*. (B) Experimental diffraction intensity on the observed layer lines in the X-ray fiber diffraction pattern of sP4MH and comparison with the lowest order Bessel functions that contribute to the calculated diffraction intensity on the layer lines for the 12/5, 17/7 and 22/9 helices. For these helices the distribution of the lowest order Bessel functions is in qualitative agreement with the experimental distribution of intensity on the layer lines. For helices with incommensurable *P* and *p* parameters the observed layer lines may be indexed according to infinite schemes, and the solutions n. 2 and 3 (17/7 and 22/9 helices) correspond to distorted 12/5 (= 2.4) helices.

Table 4. Comparison of Possible Indexing Schemes of Layer Lines for Syndiotactic Poly(4-methyl-1-hexene) (sP4MH)

experimental		12/5 helix, c = 48.3$_6$ Å, P/p = 2.40		17/7 helix, c = 68.5$_5$ Å, P/p = 2.429		22/9 helix, c = 88.7$_1$Å, P/p = 2.444		
ζ_{obs} (Å^{-1})^a	I_{obs} ^{b}	l	ζ_{calc} (Å^{-1})^a	l	ζ_{calc} (Å^{-1})^a	l	ζ_{calc} (Å^{-1})^a	n^c
0	s	0	0	0	0	0	0	0
0.045	w	2	0.041$_3$	3	0.043$_8$	4	0.045$_1$	−2
0.056	m	3	0.062$_0$	4	0.058$_3$	5	0.056$_4$	+3
0.091	w	4	0.082$_7$	6	0.087$_5$	8	0.090$_1$	−4
0.101	s	5	0.103$_3$	7	0.102$_1$	9	0.101$_4$	+1
0.147	vs	7	0.144$_7$	10	0.145$_9$	13	0.146$_5$	−1
0.159	w	8	0.165$_4$	11	0.160$_4$	14	0.157$_8$	+4
0.202	s	10	0.206$_8$	14	0.2042	18	0.202$_9$	+2

^{a} Observed values of the cylindrical coordinate ζ (ζ_{obs}) of the different layer lines in the X-ray fiber diffraction pattern of sP4MH, and values calculated (ζ_{calc}) for helices 12/5, 17/7, and 22/9 ^{b} Average value of the experimental diffraction intensity observed on the various layer lines *l* of the X-ray fiber diffraction pattern of sP4MH. Key: vs = very strong, s = strong, ms = medium strong, m = medium, and w = weak. ^{c} Value of the lowest order *n* of the Bessel functions that contribute to the diffraction intensity on the corresponding layer line at the value of ζ_{calc}.

1 in Figure 6) and therefore they also correspond to a similar distribution of the lowest order Bessel function on the layer lines along the ζ coordinate. The three reliable indexing schemes are also reported in Table 4. The experimental values of the height of the layer lines ζ_{obs} observed in the X-ray fiber diffraction pattern of sP4MH are compared in Table 4 with those calculated for the 12/5, 17/7 and 22/9 helices. This comparison allows identifying the 22/9 (or 22/13) helix as a reasonable commensurable approximation for the conformation of the chains of sP4MH in the crystals.

Concluding Remarks

A practical method for the determination of the best *M* and *N* helical parameters of complex helices from fiber diffraction data has been presented. Depending on the degree of accuracy of experimental diffraction data suitable commensurate

approximate values of M and N parameters may be found even in the case of distorted helices where the true P/p ratio is an irrational number. The method allows for a ready identification of the parent undistorted approximate helix, that is, the simplest helix with low M and N integer parameters that gives a diffraction intensity distribution on the layer lines in closest agreement with the experimental distribution of intensity observed in the X-ray fiber diffraction pattern. With respect to the literature methods proposed so far, our method has the advantage of being more suitable for its implementation in a software work-package aimed at solving helical structures. The graphical representation of the method is also less demanding and laborious than Mitsui's method. The method is very simple and can be used also by nonspecialists in diffraction analysis of crystalline polymers or even for didactical purposes.

Acknowledgment. This work was supported by Seven Framework Programme, Project No. 218331 NaPolyNet.

References and Notes

(1) Pauling, L; Corey, R. B. *Proc. Natl. Acad. Sci. U.S.A.* **1951**, *37*, 235.
(2) Watson, J. D.; Crick, F. H. C. *Nature (London)* **1953**, *171*, 737.
(3) Arnott, S.; Mitra, A. In *Molecular biophysics of the extracellular matrix*; Arnott S., Rees D. A., Morris E. R., Eds.; Humana Press: New Jersey, 1984; pp 41−67.
(4) (a) Astbury, W T; Street, A. *Philos. Trans. R. Soc. London A* **1931**, *230*, 75. (b) Astbury, W. T.; Bell, F. O. *Tabul. Biol.* **1939**, *17*, 90.
(5) (a) Ramachandran, G. N.; Kartha, G. *Nature (London)* **1955**, *176*, 593. (b) Rich, A.; Crick, F. H. C. *Nature (London)* **1955**, *176*, 915.
(6) (a) Pauling, L.; Corey, R. B. *Proc. Natl. Acad. Sci. USA.* **1953**, *39*, 247. (b) Pauling, L.; Corey, R. B. *Proc. Natl. Acad. Sci. U.S.A.* **1953**, *39*, 253. (c) Struik, D. J. *Lectures on Classical Differential Geometry* Dover: New York, 1988; (d) Cahill, K. *Phys. Rev. E* **2005**, *72*, 062901.
(7) Holmes, K. C.; Popp, D.; Gebhard, W.; Kabsch, W. *Nature (London)* **1990**, *347*, 44.
(8) Squire, J. M.; Al-Khayat, H. A.; Yagi, N. *J. Chem. Soc. Faraday Trans.* **1993**, *89*, 2717.
(9) (a) Cohen, C.; Harrison, S. C.; Stephens, R. E. *J. Mol. Biol.* **1971**, *59*, 375. (b) Nogales, E.; Whittaker, M.; Milligan, R. A.; Downing, K. H. *Cell* **1999**, *96*, 79.
(10) (a) Inouye, H.; Fraser, P. E.; Kirschner, D. A. *Biophys. J.* **1993**, *64*, 502. (b) Malinchik, S. B.; Inouye, H.; Szumowski, K. E.; Kirschner, D. A. *Biophys. J.* **1998**, *74*, 537.
(11) (a) Yamashita, I.; Vonderviszt, F.; Mimori, Y.; Suzuki, H.; Oosawa, K.; Namba, K. *J. Mol. Biol.* **1995**, *253*, 547. (b) Yamashita, I.; Hasegawa, K.; Suzuki, H.; Vonderviszt, F.; Mimori-Kiyosue, Y.; Namba, K. *Nat. Struct. Biol.* **1998**, *5*, 125. (c) Marvin, D. A.; Wiseman, R. L.; Wachtel, E. J. *J. Mol. Biol.* **1974**, *82*, 121. (d) Goldstein, R. E.; Goriely, A.; Huber, G.; Wolgemuth, C. *Phys. Rev. Lett.* **2000**, *84*, 1631.
(12) (a) Franklin, R. E.; Klug, A. *Acta Crystallogr.* **1955**, *8*, 777. (b) Barrett, A. N.; Leigh, J. B.; Holmes, K. C.; Leberman, R.; Sengbusch, P.; Klug, A. *Cold Spring Harbor Symp. Quant. Biol.* **1971**, *36*, 433. (c) Gregory, J.; Holmes, K. C. *J. Mol. Biol.* **1965**, *13*, 796. (d) Namba, K.; Pattanayak, R.; Stubbs, G. *J. Mol. Biol.* **1989**, *208*, 307. (e) Namba, K.; Stubbs, G. *Acta Crystallogr.* **1985**, *A41*, 252. (f) Stubbs, G. J.; Diamond, R. *Acta Crystallogr.* **1975**, *A31*, 709.
(13) Frette, V.; Tsafrir, I.; Guedeau-Boudeville, M.-A.; Kandel, D.; Stavans, J. *Phys. Rev. Lett.* **1999**, *83*, 2465.
(14) Goriely, A.; Tabor, M. *Phys. Rev. Lett.* **1998**, *80*, 1564.
(15) (a) Corradini P. In *Stereochemistry of Macromolecules*; Ketley, A., Ed.; Marcel Dekker: New York, Part III, 1968; p 1.; (b) De Rosa, C. In Materials Chirality: Topics in Stereochemistry; Green, M. M., Nolte, R. J. M., Meijer, E. W., Eds.; John Wiley and Sons: Hoboken, NJ, 2003, 24, 71.
(16) (a) Sperati, C. A.; Starkweather, H. W.Jr. *Fortschr. Hochpolym. Forsch.* **1961**, *2*, 465. (b) Pierce R. H. H. Jr.; Clark, E. S.; Withney, J. F.; Bryan, W. M. D. *Abstracts of Papers, 130th Meeting of American Chemical Society, Atlantic City, NJ*; American Chemical Society: Washington, DC, 1954; p 9. (c) Bunn, C. W.; Howells, E. R. *Nature* **1954**, *174*, 437. (d) Clark, E. S.; Muus, L. T. *Z. Kristallogr.* **1962**, *117*, 119. (e) Clark, E. S. *Bull. Am. Phys. Soc.* **1973**, *18*, 317. (f) Clark, E. S. *Polymer* **1999**, *40*, 4659.
(17) See for instance: Tadokoro, H. *Structure of Crystalline Polymers*; John Wiley & Sons: New York, 1979.
(18) Bamford, C. H.; Elliott, A.; Hanby, W. E. *Synthetic Polypeptides*; Academic Press: New York, 1956; p 241.
(19) Cochran, W.; Crick, F. H. C.; Vand, V. *Acta Crystallogr.* **1952**, *5*, 581.
(20) Stokes, A. R. *Prog. Biophys. Biophys. Chem.* **1955**, *5*, 140–67.
(21) (a) Mitsui, Y. *Acta Crystallogr.* **1966**, *20*, 694. (b) Mitsui, Y. *Acta Crystallogr.* **1970**, *A26*, 658.
(22) (a) Zambelli, A.; Grassi, A.; Galimberti, M.; Perego, G. *Makromol. Chem. Rapid. Commun.* **1992**, *13*, 269. (b) *Makromol. Chem. Rapid. Commun.* **1992**, *13*, 467.
(23) Knupp, C; Squire, J. M. *J. Appl. Crystallogr.* **2004**, *37*, 832. The free download of the program HELIX is available at the CCP13 website (http://www.ccp13.ac.uk).
(24) Bassi, I. W.; Bonsignori, O.; Lorenzi, G. P.; Pino, P.; Corradini, P. *J. Polym. Sci., Polym. Phys. Ed.* **1971**, *A2*, 193.